Effects of Causal Networks on the Structure and Stability of Resource Allocation Trait Correlations

By: Robert P. Gove, William Chen, Nicholas B. Zweber, Rebecca Erwin, Jan Rychtář, David L. Remington

Gove, R.P., W. Chen, N.B. Zweber, R. Erwin, J. Rychtář, and D.L. Remington. 2012. Effects of causal networks on the structure and stability of resource allocation trait correlations. Journal of Theoretical Biology 293:1-14. doi:10.1016/j.jtbi.2011.09.034

Made available courtesy of Elsevier: http://www.dx.doi.org/10.1016/j.jtbi.2011.09.034

Abstract:

Discovering the mechanisms by which genetic variation influences phenotypes is integral to understanding life-history evolution. Models describing causal relationships among traits in a developmental hierarchy provide a functional basis for understanding the correlations often observed among life-history traits. In this paper, we evaluate a developmental network model of life-history traits based on the perennial herb Arabidopsis lyrata, evaluate phenotypic, genetic, and environmental covariance matrices obtained under different scenarios of quantitative trait locus (QTL) effects in simulated crosses, test the efficacy of structural equation modeling to identify the correct basis for multiple-trait QTL effects, and compare model predictions with field data. We found that the trait network constrained the phenotypic covariance patterns to varying degrees, depending on which traits were directly affected by QTLs. Genetic and environmental covariance matrices were strongly correlated only when direct QTL effects were spread over many traits. Structural equation models that included all simulated traits correctly identified traits directly affected by QTLs, but heuristic search algorithms found several network structures other than the correct one that also fit the data closely. Estimated correlations among a subset of traits in F2 data from field studies corresponded closely to model predictions when simulated QTLs affected traits known to differ between the parental populations. Our results show that causal trait network models can unify several aspects of quantitative genetic theory with empirical observations on genetic and phenotypic covariance patterns, and that

incorporating trait networks into genetic analysis offers promise for elucidating mechanisms of life history evolution.

Keywords: Life-history evolution | G-matrix | Trait network | Path models | Arabidopsis lyrata

Article:

1. Introduction

Discovering the mechanisms by which genetic variation gives rise to variation in life-history traits is integral to understanding the nature and patterns of phenotypic evolution. Life-history traits (i.e. those related to survival and the timing and patterns of growth and reproduction) contribute directly or indirectly to fitness, and are often phenotypically and genetically correlated with each other due to processes such as resource allocation trade-offs (Stearns, 1992). Traditional quantitative genetic approaches in evolutionary biology have focused on the genetic variance‐covariance matrix of a set of traits (or **G**-matrix) as a primary tool to predict the evolutionary potential of a population under selection (Arnold et al., 2008, Kelly, 2009, Lande, 1979, Lande, 1980 and Lande and Arnold, 1983). Genetic covariances can either facilitate or interfere with natural selection on a set of traits, depending on the sign and strength of the covariances and the nature of the traits' relationship to fitness (see Arnold et al., 2008 for a recent discussion). For example, if two traits that are positively correlated with fitness (e.g. fecundity and lifespan, or number vs. size of offspring) have negative genetic covariances with each other, then it will be difficult to select simultaneously for increases in both.

While quantitative genetic approaches can be highly useful for predicting evolutionary trajectories, genetic correlations alone tell us little about the functional mechanisms underlying multiple-trait variation and evolution. Different combinations of pleiotropic effects among genes can lead to similar trait correlations but produce drastically different degrees and patterns of correlated response to selection (Gromko, 1995). Developmental hierarchies and genetic variation in resource acquisition can result in positive genetic correlations even when functional trade-offs are present (Björklund, 2004, Houle, 1991, van Noordwijk and de Jong, 1986 and Worley et al., 2003). A developmental perspective, taking into account the hierarchies in which multiple-trait variation is expressed and how it is shaped by environmental variation, has the potential to provide a better-resolved functional understanding of phenotypic evolution (Pigliucci, 2005, Pigliucci, 2007, Schlichting and Pigliucci, 1998, Stearns et al., 1991 and Willmore et al., 2007).

Developmental hierarchies introduce a complex set of inter-trait relationships into the multivariate partitioning between genetic and environmental sources of variance (Atchley and Hall, 1991). Developmental cascades lead to both genetic and environmental correlations even in the absence of direct pleiotropy (i.e. pleiotropic effects of allelic variants in genes that act independently in multiple tissues or developmental stages) and direct common-environment effects. Moreover, the genetic and environmental covariances will be correlated with each other

because both include the partial regression coefficients of the causal relationships between the traits (see Appendix A). It has long been recognized that genetic and environmental variation can influence multiple traits through the same developmental pathways, leading to similar genetic and environmental covariance patterns (Cheverud, 1996, Hegmann and DeFries, 1970 and Lande, 1979). Systematic genetic correlations induced by developmental processes ("structured" or "constrained" pleiotropy) thus represent functional constraints on patterns of trait variation that can limit the range of trait evolution (de Jong, 1990, Lande, 1979 and Wagner, 1989) and possibly explain the high degree of similarity often found between genetic and phenotypic correlation matrices (Cheverud, 1996, Roff, 1997 and Steppan et al., 2002).

Path models provide an intuitive tool for interpreting patterns of variation in life-history traits in the context of potentially causal developmental mechanisms and quantitative trait locus (QTL) effects on individual traits. Path analysis methods were initially developed by Wright, 1918 and Wright, 1921 as a method to interpret correlations in biological data in terms of potential causal models. Path analysis is now typically carried out using structural equation modeling (SEM) methods, and provides a potentially more insightful alternative to the more traditional Fisherian approaches to variance partitioning for interpreting quantitative genetic data (Lynch and Walsh, 1998). Life-history traits are connected in a developmental network of causal relationships, with "upstream" traits expressed early in development (e.g. resource acquisition) affecting subsequent traits that are "downstream" in developmental hierarchies (e.g. reproductive output), and with trade-offs in the form of resource allocation to multiple tissues or functions (Björklund, 2004, van Noordwijk and de Jong, 1986 and Worley et al., 2003). Consequently, life-history hierarchies and their relationships to fitness lend themselves well to path analysis (Atchley and Hall, 1991, Crespi and Bookstein, 1989, Li et al., 2006, Mitchell-Olds and Bergelson, 1990, Mitteroecker and Bookstein, 2007 and Scheiner et al., 2000). Nevertheless, path models have seen limited use for interpreting patterns of quantitative genetic variation in a causal framework. The primary exception is the increasing use of SEM or Bayesian networks in systems biology to infer gene regulatory networks from QTL effects on transcript abundance in genetic crosses (recently reviewed by Mackay et al., 2009 and Rockman, 2008). Such "genetical genomics" or "systems genetics" experiments, however, typically capture global transcript abundance data at a single point in time and often from a single tissue, not morphological and life-history variation over a developmental hierarchy.

In this paper, we first examine the properties of the family-level covariance structure of life-history traits generated by a causal network, using a model based on resource allocation traits in the perennial and highly variable herbaceous rosette plant *Arabidopsis lyrata*. Based on the reasoning described above, we examined two related hypotheses: (a) the developmental constraints imposed by the causal network would lead to phenotypic buffering, in which the phenotypic covariance patterns would be similar regardless of which traits were being directly affected by genetic variation, and (b) genetic and environmental covariance matrices would be correlated with each other, especially when QTL effects were either distributed among many

traits or when direct QTL effects were limited to “upstream” traits (i.e. those generally functioning relatively early in the causal network). To test these hypotheses, we constructed a developmental trait network model for life-history traits. This model was based on observations and field study data on seasonal developmental patterns in *A. lyrata*, combined with trade-off theory that took into account potential meristem- and physiologically-based mechanisms. We simulated F_2 families with and without segregating QTLs directly affecting specified traits or trait combinations. We evaluated the extent and significance of differences between the phenotypic covariance matrices generated under a null scenario of no genetic variation vs. scenarios with genetic effects on different traits or trait combinations. We also partitioned the phenotypic matrix into genetic and environmental components and evaluated the degree of similarity between the genetic and environmental covariance matrices (**G** and **E**, respectively).

Second, we examined the efficacy of structural equation models for inferring the causal basis for QTL effects in the underlying trait networks. We tested whether SEMs specifying the correct causal structure of QTL-trait effects fit the covariance structure of simulated datasets better than those in which the model was misspecified, including whether SEMs based on an incomplete set of the simulated traits produced results consistent with the correct causal structure.

Finally, we evaluated the realism of the correlation patterns generated by the trait network model. This was tested by comparing correlation matrices generated from simulated data with those estimated from field study data for progeny of a cross between *A. lyrata* parents with divergent resource allocation patterns.

2. Methods

2.1. Model organism

We developed a trait network model based on developmental and life history patterns in *Arabidopsis lyrata*(L.) O'Kane and Al-Shehbaz (Brassicaceae), a useful model plant for studying the genetic and developmental basis for life history variation. *A. lyrata* is a perennial rosette plant with a patchy distribution across northern Eurasia (ssp. *petraea*) and North America (ssp. *lyrata*) (Clauss and Koch, 2006, Leinonen et al., 2009 and Riihimäki et al., 2005). In eastern North America, populations of ssp. *lyrata* extend south along the Appalachian Mountains into the southern states, and occasionally into the adjacent foothill regions. *A. lyrata*occurs generally on rocky or sandy sites with low levels of vegetative competition, such as rock outcrops, river banks, and sand dunes (Clauss and Koch, 2006). Seeds typically germinate in late summer or fall and the plant develops a primary vegetative rosette of leaves on an unelongated main shoot. The reproductive phase begins the following spring or summer with elongation (bolting) of the main shoot to produce an indeterminate flowering shoot, which may become branched. Axillary meristems from the primary rosette may develop as sessile lateral vegetative shoots, resulting in a branched rosette, or as additional flowering shoots (Fig. 1a and b). Flowers are insect pollinated and develop into capsule-like fruits called siliques, each of

which may produce 5-40 seeds. Lateral vegetative rosettes persist overwinter and repeat the cycle described above for the primary rosette in subsequent years (Clauss and Koch, 2006 and Leinonen et al., 2009). Many aspects of the *A. lyrata* life history are likely to be shared among a wide variety of herbaceous perennial plants, making it a useful model for understanding perennial plant life history evolution.

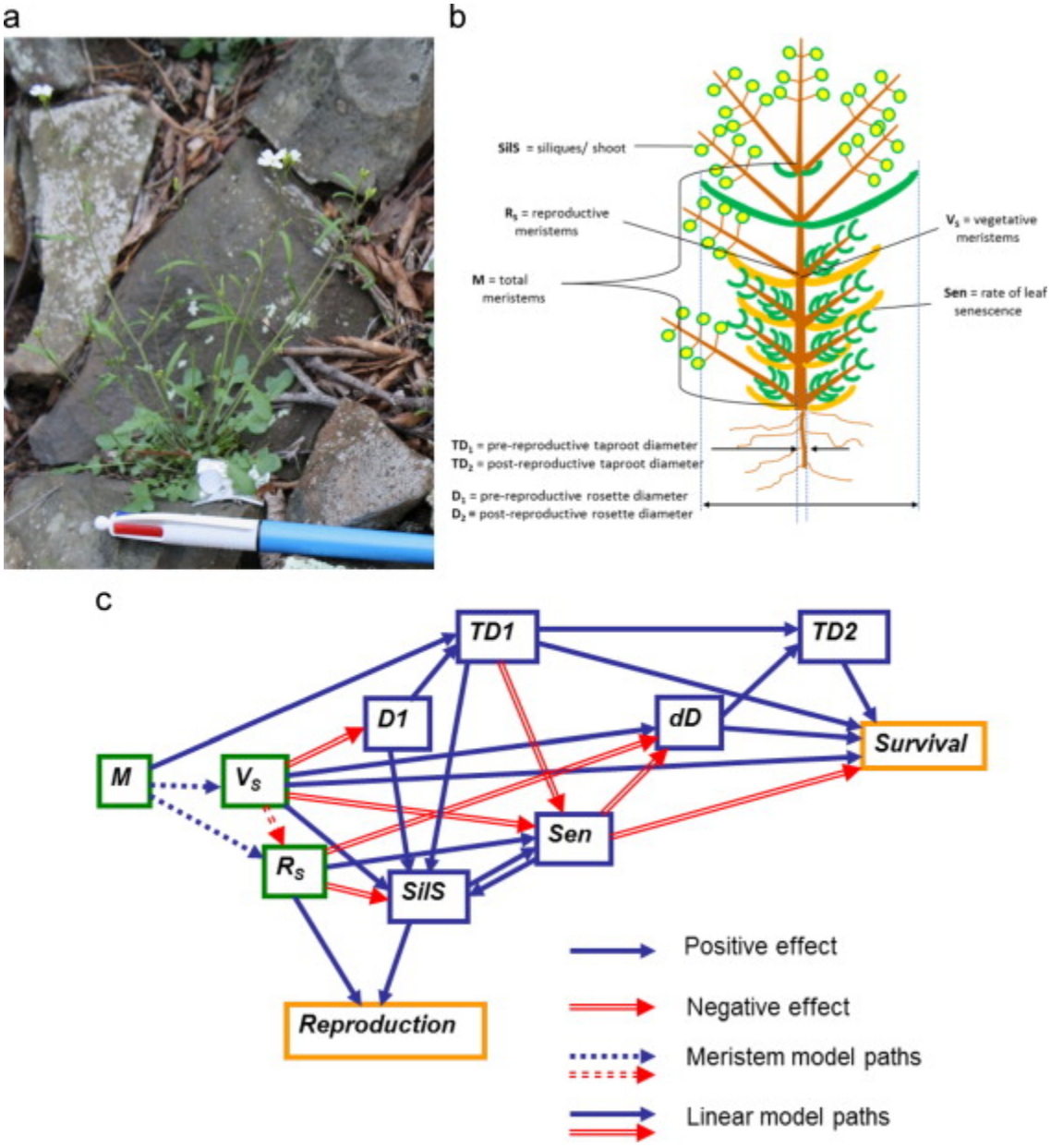

Fig. 1. Developmental trait network model for *Arabidopsis lyrata* life-history traits. (a) Flowering *A. lyrata*, Mayodan, NC, USA. (b) Schematic of flowering *A. lyrata* showing plant structure and illustrating the traits included in the trait network model. (c) Trait network model diagram. Traits corresponding to the symbols in boxes are shown in Table 1. Meristem traits are shown in green boxes, non-meristem traits in blue boxes, and fitness measures in orange boxes.

Arrows represent cause‐effect mechanisms (for interpretation of the references to colour in this figure legend, the reader is referred to the web version of this article).

We have observed that *A. lyrata* populations from different regions growing in common garden sites show substantial differences in resource allocation patterns, primarily manifested as trade-offs between the amount of flowering (numbers of flowering shoots and numbers of siliques per shoot) and net vegetative growth during the flowering period (Leinonen et al., 2009; P.H. Leinonen, D.L. Remington, and O. Savolainen, unpublished data). These patterns may represent adaptation to the wide range of environments experienced by different *A. lyrata* populations, which occur in climates that range from alpine subarctic to warm, humid temperate.

2.2. Trait network development and assumptions

To construct a developmental trait network model for *A. lyrata* life history, we identified ten potentially measurable traits that represent developmental features expressed over a single season and that could presumably be directly affected by genetic variation (Table 1). Next, we developed predictions for direct positive or negative cause‐effect relationships between traits (Fig. 1c). Mechanisms included (a) allocation of axillary meristems to alternate fates (vegetative, reproductive, or remaining latent); (b) acquisition of resources, primarily represented by pre-flowering rosette diameter as a surrogate for vegetative biomass and by vegetative meristem allocation; (c) allocation of physiological resources to alternate uses, which result in limitations on the availability of resources for contemporaneous or subsequent uses; (d) resource storage, primarily in roots (represented by root collar diameter, which can be measured non-destructively); and (e) recycling of resources from root storage or through sacrifice of leaves. Reproductive output and survival probability to the next season were included as functions of the reproductive allocation and vegetative allocation traits, respectively, to describe how the trait network is expected to affect fitness, but we do not explore these relationships in the current study. The rationale for each predicted cause‐effect relationship is explained in Appendix B.

Table 1. Traits included in the developmental trait network model.

Symbol	*Trait description*	*Distribution*
M	Total number of meristems (primary+axillary)	Poisson
VS	Number of axillary vegetative shoots	Poisson
RS [a]	Number of flowering (reproductive) shoots	Poisson
D1 [a]	Pre-flowering rosette diameter	Normal
TD1	Pre-flowering taproot diameter	Normal
SilS [a]	Number of siliques per flowering shoot	Normal
Sen	Rate of leaf senescence	Normal
dD [a]	Net rosette diameter change during flowering	Normal
TD2	Post-flowering taproot diameter	Normal

a Basic resource allocation traits used in model comparisons.

While most of the predicted relationships are logically derived from general resource allocation theory (de Jong and van Noordwijk, 1992, Koelewijn, 2004, Stearns, 1992 and van Noordwijk and de Jong, 1986), some are based on specific observations of *A. lyrata* development from field and growth chamber studies of different populations. First, the directional hierarchical relationship between axillary vegetative and reproductive shoots was based on the observation that axillary vegetative shoots begin development prior to flowering. For simplicity, our model assumed that axillary vegetative shoots do not generally switch to become reproductive during the current season and that the switch to reproduction on any shoot is irreversible, both of which may not be true in all cases. Similar but not identical patterns of development have been described in another perennial Brassicaceae species, *Arabis alpina* (Wang et al., 2009). Second, our observations suggested that axillary vegetative shoots have much smaller leaves than those growing from the primary shoot. Thus, as older large primary leaves die, plants with extensive axillary vegetative development tend to have more compact crowns with smaller rosette diameters than those that continue to produce leaves exclusively on the primary shoot. For this reason, we modeled a negative effect of axillary vegetative shoot number on pre-flowering diameter. The path model includes one reciprocal relationship, with bidirectional paths connecting siliques per shoot and leaf senescence, as we predicted that either trait could affect the other.

F_2 data for segregating progeny (n=500 or n=5000 in the analyses reported here) were simulated using a program written in MatLab version 7.4 (MathWorks Inc., 2007). Values of all six non-meristem traits were simulated in accordance with a linear model:

equation(1)

$$Y_{ij}=\mu_j+a_j b_{ij}+\sum k\neq j Y_{ik} p_{kj}+e_{ij}$$

where *Yij* is the phenotypic value of individual *i* for trait *j*; μj is the mean trait value, *bij*=1, 0, or −1 for the genotypes Q_1Q_1, Q_1Q_2, and Q_2Q_2 in individual *i* at a quantitative trait locus (QTL) affecting trait *j*simulated in accordance with F_2 probabilities; *aj* is the additive genetic effect of the Q_1 allele; *Yik* is the phenotypic value of individual *i* for each trait $k \neq j$; *pkj* is the non-standardized path coefficient for the direct effect of trait *k* on trait *j*; and *eij* is a normally-distributed random residual environmental effect on trait *j* in individual *i*. The values of *aj* and *bij* were set to zero if there were no direct QTL effect on trait *j*. For simplicity, all non-meristem trait values were simulated with a mean of zero and a residual environmental variance of one; i.e. *uj*=0 and *eij*~*N*(0,1). It is also possible to simulate genetic effects on the path coefficients (*pkj* in Eq. (1)), which would result in genetic variation in downstream trait variances but not means. We did not explore the consequences of these kinds of effects in the present study.

The allocation of axillary meristems to alternate fates as vegetative shoots (*VS*), reproductive shoots (*RS*), or remaining latent is not well-described by the linear model in Eq. (1), so alternate meristem fates were simulated as Poisson-distributed random variables as follows:

equation(2a)

$$M_i = Poisson[\mu_M + a_M b_{iM}\sqrt{\mu_M}]$$

equation(2b)

$$V_{S_i} = Poisson[vM_i + a_v b_{iv}\sqrt{vM_i}]$$

equation(2c)

$$R_{S_i} = Poisson[r(M_i - V_{S_i}) + a_r b_{ir}\sqrt{r(M_i - V_{S_i})}]$$

where μM is the mean number of total meristems on the primary shoot, *v* is the mean proportion of total meristems that develop as vegetative shoots, and *r* is the proportion of non-vegetative meristems that develop as reproductive shoots; *biM*, *biv*, and *bir* are the indicators for simulated genotypes at QTLs directly affecting *M*, *v*, and *r*, respectively; and *aM*, *av*, and *ar* are the QTL allelic effects on *M*, *v*, and *r*, respectively. The algorithm first solved for the meristem allocation trait values, which were strictly upstream of all non-meristem traits. The meristem trait values were then standardized by subtracting the expected overall trait mean (μM for *M*, $v\mu M$ for *VS*, and $r(1-v)\mu M$ for *RS*) and dividing by the Poisson residual standard deviation (the square root of the expected mean). The values for non-meristem traits were then obtained by solving a system of linear equations corresponding to Eq. (1), using the *linsolve*command in MatLab, which is able to accommodate reciprocal and cyclical relationships among variables. Solution of these equations was simplified by the structure of the model, in which all meristem traits were strictly upstream of non-meristem traits.

The values of μM, *v*, and *r* were set at 64, 0.25, and 0.5 for all simulations, which are reasonable average values for *A. lyrata* based on our field and growth chamber data and observations. Simulated genetic effects on an individual trait were limited to a single QTL with additive effects. QTL effects on multiple traits could be simulated either as a single pleiotropic QTL or independent QTLs affecting each trait. All path coefficients (*pkj* in Eq. (1)) for effects on non-meristem allocation traits were set at 0.5 for positive effects of trait *k* on trait*j*, −0.5 for negative effects, and zero if there was no predicted direct path from trait *k* to trait *j*. The actual standardized effects deviated somewhat from these values because trait values were scaled by their environmental variances, which represented different proportions of the total variances in different traits depending on the path model and the particular genetic effects that were simulated. Standardized path coefficients with absolute values in the vicinity of 0.5 were within the range observed in empirical studies with life-history traits (Lacey and Herr, 2005 and Scheiner et al., 2000), and were also close to the midrange of estimated values we have

obtained from simplified path models constructed from observed traits in *A. lyrata*(D.L. Remington, unpublished data). All path coefficients for effects of meristem allocation traits on each other were set at zero because these effects were simulated in the meristem model prior to solving the linear model.

One hundred F_2 data sets of 5000 progeny each were simulated using the parameters described above for each of the following models (Supplementary data, Table S1): (a) a null model with no genetic variation; (b) nine models, each with a single QTL affecting one of the traits listed in Table 1 except *NS*, with a=2 residual standard deviation units for each trait except *VS* (a=3.2); (c) a model with positively-correlated pleiotropic effects of a single QTL on *M* and *SilS* (a=2 for each trait; the *M*+*SilS* Model); (d) a model with negatively-correlated pleiotropic effects of a single QTL on *VS* and *SilS* (a=3.2 and −2, respectively; the *VS*+*SilS*Model); (e) a model similar to (d) in which a was reduced to −0.75 for *SilS* (*VS*+*SilS2* Model); and (f) a model with separate QTLs affecting each trait in the network, with the value of a for each trait randomly sampled from a normal distribution with mean zero and standard deviation of 0.5 (*All* Model). The larger QTL effects on*VS* were chosen based on our observations that *A. lyrata* populations are highly variable in this trait. Additional data sets with 500 F_2 progeny were simulated under the null and *All* models.

2.3. Covariance matrix comparisons

Phenotypic variance‑covariance matrices (**P** matrices) for each simulated dataset were estimated in the MatLab simulation program for four traits: pre-flowering rosette diameter (*D1*), number of reproductive shoots (*RS*), number of siliques per shoot (*SilS*), and rosette diameter change during the flowering season (*dD*). These traits represent the basic measures of resource acquisition (*D1*) and reproductive (*RS* and *SilS*) and vegetative (*dD*) resource allocation that have been scored in *A. lyrata* field studies, and are subsequently referred to as the basic resource allocation traits.

To test whether **P** matrices of the resource allocation traits differed significantly between datasets simulated under models with QTL effects vs. the null model, we tested for common principal components among pairs of variance‑covariance matrices as implemented in the program CPC (Phillips, 1997). CPC implements likelihood ratio tests of hierarchically nested models that share different numbers of principal-component parameters, so the null hypothesis for each test is that the two models are identical in the tested component(s). The tested models, in order of increasing numbers of shared parameters, were unrelated (the full model in which all four principal components were estimated separately for each matrix): the first principal component (PC1) in common; PC1 and PC2 in common; all principal components in common; proportionality (all principal components in common with proportional eigenvalues); and equality (all principal components in common with equal eigenvalues).

To test whether pairs of **P**-matrices shared significant similarity, we used the random skewers method (Cheverud, 1996, Cheverud and Marroig, 2007 and Cheverud et al., 1983), as

implemented in the program Skewers (available from the website http://anolis.oeb.harvard.edu/~liam/programs/). In contrast with the CPC analyses, the null model in the random skewers test is that the tested models are uncorrelated. For each tested pair of matrices, 10,000 random selection vectors (skewers) were applied to both matrices, and the phenotypic response vectors to each skewer and their correlations between the two matrices were calculated. Each skewer was also applied to a pair of random response vectors, and an empirical *p*-value for matrix similarity was calculated as the frequency with which the random response vectors were more highly correlated than the actual response vectors from the two matrices. In addition to providing a test of matrix similarity, the mean correlation of response vectors for each pair of matrices provided a relative measure of similarity in predicted evolutionary response by which different pairs of variance-covariance matrices could be compared (Cheverud and Marroig, 2007).

We also used the random skewers' method to test whether the genetic and environmental variance-covariance matrices (**G** and **E** matrices, respectively) from individual simulated datasets were significantly correlated with each other. The **G** and **E** matrices were partitioned from the **P** matrix for all 100 of the 5000-progeny simulations from the *All* model and one simulation under each of the other models, using the manova function in a script written in R version 2.11.1 (R Development Core Team, 2008). Genetic effects were estimated from a regression of the multivariate phenotypic matrix on the simulated genotypes for each simulated QTL. The **G** matrix was calculated from the mean squares and cross-products for the summed QTL effects in the model, and the **E** matrix from the residual sum of squares and cross products (see Supplementary file 1 for the *R* script). By definition, there is no response to selection on **E**, which has no genetic variation. However the response vector on the **E** matrix in the random skewers analysis can be interpreted as the mean deviation in the residual multivariate phenotype, after adjustment for all genetic effects, in a set of individuals selected on the basis of an index of phenotypic values. This is completely analogous to the response vector to selection on the **G** matrix, which represents the deviation in genotypic values in a set of individuals selected on an index of phenotypic values (Cheverud, 1996 and Cheverud and Marroig, 2007).

2.4. Structural equation modeling

Structural equation models (SEM) were constructed and tested using the SEM package in *R* version 2.11.1 (Fox, 2006 and R Development Core Team, 2008). SEMs were represented by a series of reticular action model (RAM) equations: one equation describing each path in the model and one describing the residual variance of each variable with the exception of the QTL genotype(s). RAM equations were of the form A->B for model paths (where A and B are the causal and the responsive traits, respectively) or A 〈-〉 A for the residual variance of trait A. A variable name was also specified for each path coefficient or residual variance. RAM statements can also be included for covariances between variables not connected by causal paths to account for unexplained correlations, but covariances were not estimated in any of our models. The SEM is described by the matrix of path coefficients (**A** matrix) and the residual variance-covariance

matrix (SEM **P**matrix) that maximize the likelihood of the observed variance-covariance matrix. (The SEM **P** matrix should not be confused with the overall **P** matrix of phenotypic variances and covariances among traits, denoted as**S** in an SEM context.) SEMs were tested on one simulated data set from the *VS+SilS2* Model (with a pleiotropic QTL directly affecting *VS* and *SilS*). SEMs were developed sequentially from a starting model that included paths from the simulated QTL to all traits but no causal paths between traits. At each step, paths with insignificant *z* values (α=0.05) were first removed and the model was refitted. If there were no insignificant paths, the trait-to-trait path from the model with the largest modification index for the **A** matrix was added and the model was refitted. If none of the five largest modification indices represented a path in the overall trait network model, the trait network path corresponding to the largest modification index for the SEM **P** matrix was added instead. The modification indices represented the approximate improvement to the likelihood ratio chi-square value for model fit if a given path (**A** matrix) or covariance (SEM **P** matrix) not included in the model was to be added. Thus, only trait-to-trait paths represented in the actual model were tested, but all potential combinations of QTL effects on traits were tested. This process was repeated until no trait-to-trait paths remained to be added or until adding or deleting paths failed to improve the fit of the model significantly as determined by a likelihood ratio test. For each SEM, the set of path coefficients and residual variances that maximized the likelihood of the observed variance-covariance matrix was obtained. A likelihood-ratio χ^2 statistic comparing the fit of the model to that of a "saturated" model with no degrees of freedom that fully explains the observed variance-covariance matrix was calculated, and the likelihood-ratio*p*-value was estimated. Models were also compared using Akaike's Information Criterion (AIC; Akaike, 1974 and Akaike, 1987), and using unadjusted and adjusted goodness-of-fit indices (GFI and AGFI).

We also used the software package Tetrad 4.0 (Spirtes et al., 2000) to test whether the correct paths in the trait network, or other network structures with equivalent statistical support, could be found using the QTL genotype and phenotypic data alone, using the same simulation as above under the *VS+SilS2* Model. In all searches, a knowledge constraint was used to prevent the QTL genotype from being downstream of any other trait in the path. Pattern searches were conducted using beam and GES algorithms, either using the knowledge-constrained simulated data alone as input or using the data in conjunction with directed acyclic graphs generated from the LiNGAM algorithm or directed graphs generated from LiNG. With the beam algorithm, we used a beam width of 5 (where higher beam widths leading to less pruning of search states at each search step), and α-values of 0.05 and 0.005. A limitation of the LiNGAM and GES algorithms is that they are based on the assumption that the true causal structure is acyclic, unlike the actual trait network model, which contains a reciprocal relationship.

To evaluate the predictive value of SEMs when only a subset of traits was measured, abbreviated SEMs including only the basic resource allocation traits (*RS*, *SilS*, *D1*, and *dD*) were also estimated for the same simulated dataset. SEMs were fit sequentially as described above, except

that the path to be added at each step was determined by testing all remaining appropriate trait-to-trait paths among the basic resource allocation traits and adding the path that contributed the largest reduction in the χ^2 statistic for fit. Paths between the basic resource allocation traits were considered appropriate if they were present in the overall model as a single step or as multiple steps passing through unmeasured traits. In addition, *D1* was tested upstream of *RS* and *dD*, as *D1* is downstream of the unmeasured *VS* and might therefore function as a partial surrogate for the effects of *VS* on *D1* and *dD*. This stepwise addition process was repeated with the unused paths until any additional unused path did not significantly improve the model fit. In addition, abbreviated models that included a latent (unmeasured) variable were tested to evaluate whether the simulated QTL effects on *VS* and the effects of *VS* on downstream traits could be correctly inferred if *VS* was not measured directly. Model paths involving the latent variable and its residual variance were specified using RAM statements as described above. We evaluated the abbreviated path models, both with and without the latent variable, for how the missing variables affected the overall fit of the model and the causal relationships detected among the remaining traits.

2.5. Field study data

The covariance structures of the basic resource allocation traits in the simulated models were compared with those from two *A. lyrata* field studies in which these traits were measured. The design, establishment, and data collection for the field studies is described in detail elsewhere (Leinonen et al., 2011). Briefly, common-garden field plantings of *A. lyrata* were established in the summer and fall of 2005 at Spiterstulen, Norway (61° 38′ N, 8° 24′ E, altitude 1106 m), and Greensboro, NC, USA (36° 04′ N, 79° 44′ W, altitude 235 m), as part of an evolutionary genetic study of local adaptation. These plantings included outcross F_2 populations from a cross between phenotypically divergent parents from Spiterstulen, Norway (collected adjacent to the Spiterstulen study site), and Mayodan, NC, USA (36° 25′ N, 79° 58′ W, altitude 225 m). Measurements of vegetative traits, reproductive traits, and survival were collected for the 2006 growing season at Greensboro and for the 2006–2008 growing seasons in Norway. Measurements at both field sites included the four basic resource allocation traits (*D1*; *RS*; siliques per shoot, *SilS*; and *dD*). For the Spiterstulen site, only the 2006 data was used in the analyses reported here. Phenotypic variance–covariance matrices were estimated from 419 F_2 plants at Spiterstulen and 357 F_2 plants at Greensboro for which complete data were available.

The phenotypic correlations from the two field studies were compared with one simulated data set from each of the models described above, using CPC to test for significant differences in the correlation matrices and random skewers to test for significant similarities. We used correlation matrices rather than variance–covariance matrices for the random skewers analyses comparing simulated and field data, because the units of measurement for the simulated vs. measured traits were heterogeneous between traits. Thus, identical selection vectors applied to field and simulated data sets would not be equivalent if applied to non-standardized data.

3. Results

3.1. Trait variation under the null model

Simulations under the null model with no genetic variation resulted in strong correlations between the four basic resource allocation traits representing resource acquisition (pre-flowering rosette diameter, *D1*), reproductive allocation (reproductive shoots; *RS*; and siliques per shoot, *SilS*), and vegetative allocation (net rosette diameter change during flowering, *dD*; Table 2). Specifically, the null model produced trade-offs between reproductive and vegetative allocation, and also trade-offs between the two reproductive allocation traits, with more flowering shoots associated with fewer siliques per shoot. In addition, the null model produced a positive correlation between pre-flowering diameter and siliques per shoot and a negative correlation between pre-flowering diameter and vegetative allocation. The only traits that were essentially uncorrelated were pre-flowering diameter and the number of reproductive shoots. Replicate simulations under the null model showed only minor run-to-run variation, especially when the larger progeny sample size (n=5000) was used (Table 2).

Table 2. Summary of phenotypic correlations from F_2 progeny sets of n=500 (top) and n=5000 (bottom) simulated under the null model (no genetic variation). Data are the mean phenotypic correlations (above diagonals) and standard deviations (below diagonals) from 100 simulations for each sample size. Standard deviations for other models were similar in magnitude. Trait abbreviations are given in Table 1.

Trait	*Trait*			
	RS	*SilS*	*D1*	*dD*
***n*=500**				
RS	1	−0.185	0.030	−0.483
SilS	0.0413	1	0.410	−0.205
D1	0.045	0.035	1	−0.294
dD	0.032	0.040	0.041	1
***n*=5000**				
RS	1	−0.183	0.034	−0.487
SilS	0.012	1	0.407	−0.205
D1	0.014	0.011	1	−0.293
dD	0.010	0.012	0.013	1

A substantial proportion of the simulated phenotypic variation in all traits except for *M* was generated by the cause-effect relationships between traits (Supplementary data, Table S2). The proportion of phenotypic variance that was developmentally-induced ranged from 0.20 for *VS* to 0.68 for *SilS*. The traits with the highest R^2net values (*SilS*, *dD*, and *Sen*) were all directly downstream of three or more of the other traits in the model.

3.2. Effects of genetic variation

When single large-effect QTLs affecting individual traits were included in the simulations, the covariance patterns were altered to varying degrees from the null model. From a qualitative standpoint, only the models with direct QTL effects on vegetative shoots (*VS* Model), reproductive shoots (*RS* Model), or pre-flowering rosette diameter (*D1* Model) produced substantial changes in the covariances among the basic resource allocation traits (Fig. 2a). The *VS* Model introduced strong positive covariances between *D1* and *RS*, which had little correlation in the other models, and the negative covariances of *D1* and *RS* with *dD* became much stronger. The trade-offs of *RS* with *SilS* and *dD* became stronger in the *RS* Model, and the *D1* Model led to a much stronger positive covariance between *D1* and *SilS*. The *SilS* Model and the *Sen* Model caused modest increases in the trade-off between *SilS* and *dD*. Pleiotropic models with QTLs affecting either *M* or *VS* plus*SilS* induced positive covariances of *RS* with *SilS* and/or *D1*, depending on the specific model, and the*VS+SilS* Models increased the negative covariances of *SilS* and *D1* with *dD*. The mean correlations from 100 simulations under the *All* model were very similar to the null model.

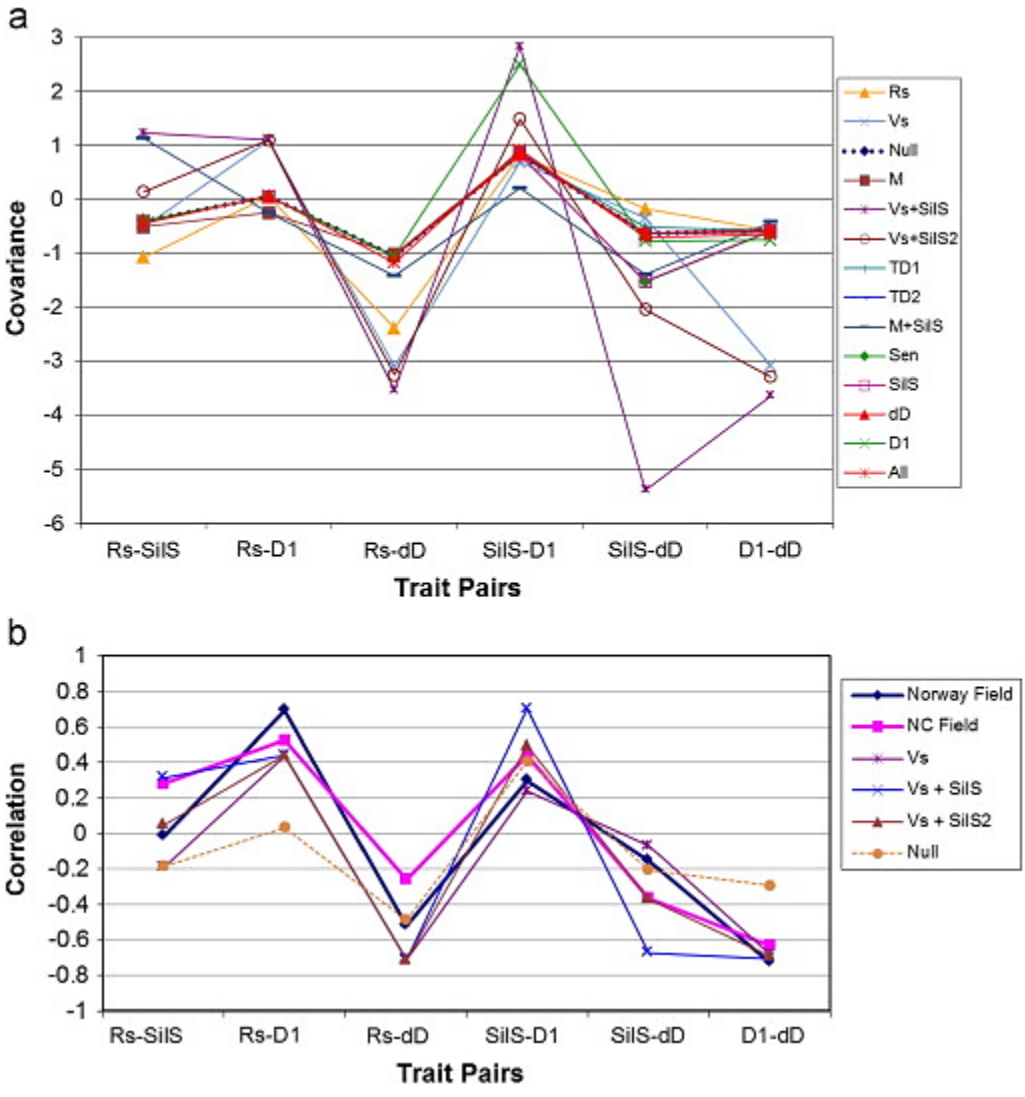

Fig. 2. (a) Comparison of trait covariances obtained with trait network simulations (mean of 100 simulations, *n*=5000) under the null model and under models in which different traits were subject to direct segregating QTL effects. (b) Comparison of trait correlations (mean of 100 simulations, *n*=5000) obtained under selected network simulations with field data from North Carolina (NC) and Norway study sites. QTL additive effects in environmental standard deviation units (*a*) are 2.0 environmental standard deviation units for all traits except *VS* (*a*=3.2) and *SilS* under the *VS+SilS* (0.75) model (*a*=0.75). Trait abbreviations are as shown in Table 1.

The first principal component (PC1) in the simulated models was generally interpretable as a trade-off between resource acquisition (*D1*) and reproductive allocation (*RS* and *SilS*) vs. vegetative (*dD*) allocation (Table 3). However, the relative PC1 loadings on the two reproductive allocation traits varied substantially between models. The *D1* Model and *SilS* Model had PC1 coefficients of nearly zero for *RS*, and the *RS* Model changed the sign of the *SilS* coefficient. PC2 generally represented a trade-off between the two reproductive allocation traits, with coefficients for the other two traits generally but not always having the same sign as that of *RS*. The PC1 and PC2 coefficients and their eigenvalues were highly stable for replicate simulations from the same model. The first principal component was significantly different from that of the null model (α <0.05) for all models except the *M*, *TD1*, and *TD2* Models in the common principal components analysis (CPC; Table 4). The *TD2* Model lacked significant differences from the null model at all hierarchical levels in the CPC analysis, which was expected because the *TD2* trait is strictly downstream from all four basic resource allocation traits in the trait network model. Results were similar when the number of simulated F_2progeny was reduced from 5000 to 500 (data not shown).

Table 3. Eigenvalues and eigenvector coefficients for the first two principal components from model simulations and field data, using the four basic resource allocation traits. Simulated data are for one representative simulation with 5000 progeny under each model scenario.

Model or data [a]	*PC1*					*PC2*				
	Eigen-value	*D1*	*Rs*	*SilS*	*dD*	*Eigen-value*	*D1*	*Rs*	*SilS*	*dD*
Null	4.216	−0.311	−0.208	−0.604	0.703	3.115	−0.122	0.502	−0.694	−0.501
D1	6.698	−0.595	−0.017	−0.746	0.300	3.476	−0.092	0.515	−0.264	−0.810
VS	11.112	−0.389	−0.369	−0.047	0.843	3.484	−0.238	0.297	−0.924	−0.031
VS+SilS	16.483	−0.320	−0.253	−0.509	0.758	3.193	−0.157	0.487	−0.755	−0.410
VS+SilS2	11.996	−0.372	−0.327	−0.262	0.829	3.413	−0.215	0.403	−0.864	−0.211
M+SilS	7.271	−0.04	−0.31	−0.85	0.40	3.122	0.007	0.512	−0.51	−0.69

		0	2	9	4				1	0
M	4.293	−0.355	−0.109	−0.684	0.628	3.332	−0.161	0.686	−0.493	−0.510
RS	5.981	−0.055	−0.684	0.173	0.706	3.989	−0.342	0.159	−0.862	0.338
Sen	5.925	−0.209	−0.112	−0.665	0.709	3.132	−0.104	0.541	−0.636	−0.541
SilS	7.441	−0.166	0.013	−0.930	0.329	3.248	0.103	0.531	−0.290	−0.790
dD	5.444	−0.181	−0.215	−0.296	0.913	3.371	−0.260	0.328	−0.871	−0.257
TD1	4.066	−0.325	−0.179	−0.650	0.663	3.310	−0.085	0.483	−0.665	−0.564
TD2	4.252	−0.331	−0.143	−0.672	0.646	3.162	−0.094	0.526	−0.619	−0.575
Field data										
Greensboro	1681.300	−0.560	−0.268	−0.087	0.779	505.130	−0.403	−0.733	−0.037	−0.547
Norway	2.349	−0.613	−0.527	−0.194	0.555	1.013	−0.052	0.349	−0.934	−0.052

a Trait(s) with direct QTL effects in model simulations. *a*=2 in residual standard deviation units for all traits except for *VS* (*a*=3.2).

Table 4. Summary of response correlations and common principal components comparisons to null model.

Simulated model (*vs. null*) [a]	*Response correlation* [b]	*P-value of CPC model comparison* [c]				
		E vs. P	*P vs. C*	*C vs. C2*	*C2 vs. C1*	*C1 vs. U*
D1	0.9477	0	0	0.2770	0	0
VS	0.9079	0	0	0.1960	0.9068	0
VS+SilS	0.9021	0	0	0.9668	0.5399	0.0008
VS+SilS2	0.9202	0	0	0.1765	0.4944	0
M+SilS	0.9145	0	0	0.0002	0.0114	0
M	0.9869	0	0	0.0003	0	**0.0545**
RS	0.9635	0	0	0.1681	0.3405	0
Sen	0.9845	0	0	0.1931	0.0902	0
SilS	0.9534	0	0	0.0442	0.1205	0
dD	0.9789	0	0	0.0014	0.0000	0
TD1	0.9989	0.8436	0.0184	0.2484	0.0145	**0.7410**
TD2	0.9996	**0.7783**	**0.9454**	**0.5067**	**0.8141**	**0.2703**

a Trait(s) with direct QTL effects. *a*=2 in residual standard deviation units for all traits except for *VS* (*a*=3.2).

b Mean of 10,000 random skewers. All reported correlations are significant (α =0.05).

c CPC Model abbreviations: *E*=equality; *P*=proportionality; *C*=all principal components in common; *C2*=first two principal components in common; *C1*=first principal component in common; *U*=unrelated (full model). Boldface *P*-values represent models that are not rejected (α =0.05) using hierarchical ("step up") criteria.

In the random skewers' comparisons, all of the single-QTL models had response vector correlations of 0.90 or greater with the null model (Table 4). All of these correlations were individually significant (α <0.05) when compared empirically to the correlations of random response vectors. The highest response correlations were for models with QTL effects on traits in relatively downstream positions in the model, except that the *M*Model, in which the trait with direct QTL effects is strictly upstream of all other traits, had one of the highest correlations with the null model.

3.3. Comparisons of **G** and **E** matrices

None of the single-QTL models showed a significant correlation between the **G** and **E** matrices in random skewers' analysis (Table 5). Contrary to our predictions, the *M* Model, in which the QTL effects are strictly upstream of all other traits, did not result in a significant correlation between the **G** and **E** matrices (Table 5;*r*=0.28, *p*=0.322). Inspection of the estimated **G** matrix from the *M* Model revealed that the genetic variances for *SilS* and *dD* were both close to zero, leading to very small genetic covariances with other traits. QTL effects on *M* generated positive genetic covariances between *VS* and *RS* in the trait network model, which in turn had opposite effects on both *SilS* and *dD* that largely canceled each other. By contrast, 81 out of 100 simulations under the *All* Model, with separate QTLs of random effect sizes affecting each trait, showed significant correlations (α =0.05) between the **G** and **E** matrices. The lowest correlation value out of the 100*All* Model simulations was 0.656, higher than the correlations for any of the single-QTL models.

Table 5. Skewers' comparison of correlations between ***G*** and ***E*** matrices in simulated datasets.

Simulated model	Correlation between ***G*** and ***E*** †	
	Correlation	*P*-value
M	0.279242	0.322
RS	0.48699	0.1955
VS	0.565908	0.1699
SilS	0.540611	0.1723
Sen	0.574336	0.1598
D1	0.453174	0.2239
dD	0.456191	0.2138
TD1	0.428803	0.242

M+SilS	0.399973	0.2464
VS+SilS	0.652123	0.1161
VS+SilS2	0.595286	0.1466
All (mean of 100 simulations)	**0.858158**	**0.0341**‡

† Analyses done with 10,000 skewers. Significant values are in boldface ($p \leq 0.05$).

‡ Correlations were significant at the $\alpha = 0.05$ level in 81 of 100 simulations.

3.4. Structural equation modeling

We used structural equation modeling (SEM) to evaluate the degree to which the QTL-trait covariance structure was informative about the underlying causal network. We fit SEMs to a complete set of genotype and trait data from a model with pleiotropic QTL effects on *VS* and *SilS* (*VS+SilS2* model). An SEM exactly matching the simulated effects, containing all trait-to-trait paths in the simulated trait network (Fig. 1) with additional paths from the QTL genotype to *VS* and *SilS*, was the only tested SEM with a strong fit to the simulated data ($\chi^2 = 26.99$, df=23, $p=0.256$, AIC=−19.01, GFI=0.999, AGFI=0.997). All path coefficients in this model were significant ($\alpha = 0.05$), and coefficients of all paths leading to non-meristem traits were close to the simulated values of 0.5 or −0.5 (Supplementary data, Table S3). Removal of any path from the SEM, including either one of the reciprocal paths connecting *SilS* and *Sen*, resulted in an SEM with a significant lack of fit. Reversing the direction of the path from *VS* to *RS*, which had the smallest estimated coefficient of any path in the model, also significantly reduced the model fit (Supplementary data, Table S4).

When we treated the trait network as unknown, with the QTL genotype constrained to be strictly causal in the network, predictions from several algorithms produced well-supported networks (Appendix C). None of the predicted networks identified the reciprocal relationship between *SilS* and *Sen*, due at least in part to the limitations of some of the algorithms used. Otherwise, each of the predicted networks contained all the paths in the actual simulated network, although the directions of some paths were sometimes reversed, and each predicted network included paths not present in the actual network. A beam search with $\alpha = 0.005$ (with or without using LiNG or LiNGAM-generated trees as search input) produced a model that differed from the true network only in missing one of the reciprocal paths between *SilS* and *Sen*, and including additional direct paths from the QTL and *D1* to *Sen* (Supplementary data; Fig. S2b).

When only the basic resource allocation traits and QTL genotypes were included in the SEM (abbreviated SEM), the best-fitting model found with a stepwise-addition approach included pleiotropic QTL effects on all four basic resource allocation traits (Fig. 3a). The signs of the estimated QTL effects on *D1*, *RS*, and *dD* were consistent with the positive coefficient of the simulated QTL effect on *VS*, which is directly upstream of each of the basic resource allocation traits. A path from *D1* to *dD*, not present in the simulated model, had a strongly negative path coefficient in the abbreviated SEM. This path was expected to occur because *D1* functions in the

abbreviated SEM as a partial surrogate for the unmeasured *VS*. *D1* is directly downstream of*VS* in the simulated model, with a negative path coefficient, and the simulated path from *VS* to *dD* is positive. This model deviated significantly but not strongly from a complete fit to the simulated covariance matrix (p=0.016; AIC=3.794; AGFI=0.993).

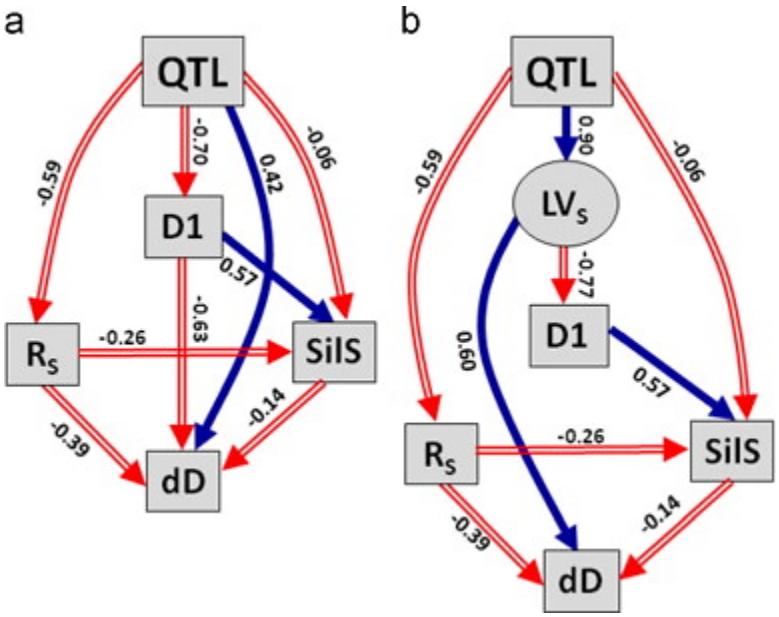

Fig. 3. Best-fitting abbreviated structural equation models (basic resource allocation traits only) including (a) QTL effects and basic resource allocation traits only, and (b) QTL effects, basic resource allocation traits, and a latent variable (*LVS*). Standardized path coefficients for each path are shown. For both models, χ^2=5.79 (1 df), p=0.016, AIC=3.79, GFI=0.999, AGFI=0.993.

We added a latent variable (*LVS*) downstream of the QTL genotypes but upstream of other traits in the abbreviated SEM to represent *VS*, which was directly affected by the QTL in the simulation used for this analysis. The best-fitting SEM we found under this scenario was statistically equivalent to the abbreviated SEM lacking the latent variable (Fig. 3b), with *LVS* replacing the effects of *D1* on *dD* and the effects of the QTL on *D1* and *dD*. This SEM included direct QTL effects on *RS* in addition to *SilS* and *LVS*. The value of *RS*is dependent on total meristems (*M*), both directly and indirectly through the effects of *M* on *VS* (Eqs. (2b) and(c)). Thus, the detected QTL effect on *RS* may be due to the joint dependency of *VS* and *RS* on *M*, which was not represented in the abbreviated model. Removing the QTL effect on *RS* and adding a path from the latent variable to *RS*, which would be structurally more consistent with the simulated model, resulted in an SEM with a substantially poorer fit (AIC=58.37; AGFI=0.928). The predicted effects of the QTL on the latent variable were almost identical to those on *VS* in the SEM on the full network (standardized coefficient of 0.89 vs. 0.90), but the predicted QTL effects on *SilS* were greatly reduced (standardized coefficients of −0.06 vs. −0.29).

3.5. Comparisons of simulated vs. field data

If the trait network model were to describe realistic aspects of causal relationships among traits in *A. lyrata*, we predicted that the correlation matrices between simulated and field data would show significant similarities. Secondly, since population data from the field sites show that the Spiterstulen and Mayodan populations are strongly differentiated genetically for the basic resource allocation traits (Leinonen et al., 2011), we predicted that at least some simulations incorporating QTL effects would provide a better fit to the field data than the null model does.

The basic resource allocation traits in the two field datasets showed similar correlation patterns to the simulated data under the null model and most of the models with single-trait direct QTL effects. However, the correlation between reproductive shoots and pre-flowering rosette diameter was strongly positive in both field datasets, and the correlation between the two reproductive allocation traits (reproductive shoots and siliques per shoot) was positive rather than negative in the Greensboro data (Fig. 2b). PC1 showed similar trade-off patterns in the field data to those in the simulations, though the PC1 eigenvectors for both sets of field data were significantly different from those of all simulations except for the Norway-*VS* model comparison (Table 6). The two sets of field data were highly similar to each other in random skewers' response vectors (response correlation=0.96). Both sets of field data showed significant response-vector similarities to all simulated datasets. Both sets of field data showed somewhat higher response similarities to the *VS* and*VS+SilS2* Models than to the null model, and the Greensboro data also showed higher response similarities to the *VS+SilS* and *TD1* Models than to the null model. The models that included QTL effects on *VS* were unique in replicating the moderately strong positive correlation observed between *RS* and *D1* found in both sets of field data, and the *VS+SilS* Model (which was developed with prior knowledge of the correlation structure of the Greensboro but not the Norway field data) showed the positive correlation between *RS* and*SilS* found in the Greensboro data.

Table 6. Summary of matrix correlations and common principal components comparisons to Greensboro field data.

Model [a]	*Response correlation* [‡]	*P-value of model comparison* [b]			
		P vs. C	*C vs. C2*	*C2 vs. C1*	*C1 vs. U*
Greensboro vs.					
Null	0.9057	<0.0001	<0.0001	<0.0001	<0.0001
D1	0.9000	<0.0001	0.6849	<0.0001	<0.0001
VS	0.9204	<0.0001	<0.0001	0.0321	<0.0001
VS+SilS	0.9224	<0.0001	<0.0001	<0.0001	0.0061
VS+SilS2	0.9352	<0.0001	<0.0001	0.0002	0.0185
M+SilS	0.8880	<0.0001	0.0054	<0.0001	<0.0001
M	0.8689	<0.0001	0.0011	<0.0001	<0.0001
RS	0.8558	<0.0001	0.0015	<0.0001	0.0001

Sen	0.9120	<0.0001	0.0013	<0.0001	0.0004
SilS	0.9065	<0.0001	<0.0001	<0.0001	<0.0001
dD	0.9063	<0.0001	0.7998	<0.0001	0.0011
TD1	0.9232	<0.0001	0.0662	<0.0001	<0.0001
TD2	0.8895	<0.0001	<0.0001	<0.0001	<0.0001
Norway vs.					
Null	0.8924	<0.0001	0.1262	<0.0001	<0.0001
Greensboro	0.9592	<0.0001	0.0283	0.6370	0.0013
D1	0.8773	<0.0001	<0.0001	<0.0001	<0.0001
VS	0.9769	<0.0001	0.0016	0.0369	0.0726
VS+SilS	0.8925	<0.0001	<0.0019	<0.0001	<0.0001
VS+SilS2	0.9549	<0.0001	0.0025	<0.0001	0.0001
M+SilS	0.8173	<0.0001	<0.0001	0.3180	<0.0001
M	0.8316	<0.0001	0.0352	<0.0001	<0.0001
RS	0.8736	<0.0001	0.4117	<0.0001	<0.0001
Sen	0.8820	<0.0001	0.1177	<0.0001	<0.0001
SilS	0.8888	<0.0001	0.5327	<0.0001	<0.0001
dD	0.8807	<0.0001	0.0688	<0.0001	0.0003
TD1	0.8963	<0.0001	0.1970	<0.0001	<0.0001
TD2	0.8702	<0.0001	0.2472	<0.0001	<0.0001

a Trait(s) with direct QTL effects. a=2 in residual standard deviation units for all traits except for *VS* (a=3.2).

b Model abbreviations: *P*=proportionality; *C*=all principal components in common; *C2*=first two principal components in common; *C1*=first principal component in common; *U*=unrelated (full model).

‡ Mean of 10,000 random skewers. All response correlations are significant ($p \leq 0.05$).

4. Discussion

4.1. Effects of developmental networks on stability of trait correlations

We hypothesized that developmental networks with cause‑effect relationships among traits would have a stabilizing effect on trait covariances. The stabilizing effect is predicted to occur because the effect of variation in a developmentally upstream trait on a downstream trait (reflected in the $Y_{ik}p_{kj}$ terms in our model; Eq. (1)) is the same whether the source of variation in the upstream trait is genetic or environmental. In accordance with this hypothesis, our simulation results showed strong and somewhat stable patterns of multiple-trait phenotypic correlations, including trade-offs in vegetative vs. reproductive resource allocation. Even large segregating single-gene direct effects on some individual traits resulted in relatively minor changes in the phenotypic covariance matrix relative to that of a null model with no genetic variation, as reflected by stability in trade-off patterns and predicted selection responses. Nevertheless, the strengths and in some cases signs of the pairwise trait correlations differed substantially among

models, as shown by the common principal component analyses. These results suggest that phenotypic buffering imposed by developmental networks is far from absolute.

The hypothesized strong correlations between **G** and **E** matrices were not found for most models. Notably, the weakest correlation was found with the *M* Model, in which the QTL effects were on the trait farthest upstream in the network. Our conceptual hypothesis was that the common transmission of genetic and environmental variation from *M* to the rest of the network would lead to relatively strong correlations between**G** and **E** in the *M* Model. Instead, we found that effects transmitted through multiple paths largely canceled each other out, leading to a near-absence of genetic variance on some downstream traits. Our results show that the effects of causal networks on the **G**-matrix may be difficult to generalize due to the complexity induced by a large number of paths.

Nevertheless, for biologically realistic situations in which genetic variation is likely to be due to the effects of many loci distributed among many traits, developmental networks may result in **G** and **E** matrices that are highly similar (Cheverud, 1996, Hegmann and DeFries, 1970 and Lande, 1979). Evidence for this is provided by the significant correlations between **G** and **E** in most of the *All* Model simulations, in which QTL effects were distributed among many traits. However, segregation at large-effect QTLs could result in large changes in **G**, depending on which traits are directly affected by the QTLs, the size and distribution pattern of QTL effects, and the detailed structure of the causal model. Moreover, relatively stable phenotypic covariance patterns can occur due to the large influence of developmentally-induced covariance patterns in the **E**-matrix even if the **G**-matrix is highly variable. For example, the phenotypic covariance structures of the *M* Model simulations (**G**+**E**) were highly similar to those of the null model (**E** only) even though **G** and **E** were poorly correlated under the **M** Model.

Our results also suggest that a developmental trait network concept can serve to unify several aspects of theory and empirical data on multivariate quantitative trait variation. In empirical studies, the genetic, environmental, and phenotypic variance‑covariance matrices are often found to be highly correlated (Cheverud, 1996). It has long been speculated that these correlations occur because traits are related through physiological or developmental mechanisms (Cheverud, 1996, Hegmann and DeFries, 1970 and Lande, 1979). Transmission of both genetic and environmental sources of variation to downstream traits through the same paths in a causal trait network provides such a mechanism. The transmission of genetic effects through the trait network also represents a mechanism to generate stable pleiotropic effects both in new mutational variation and standing genetic variation. Stable pleiotropic patterns of mutational variation are a factor that can favor **G**-matrix stability (Cheverud, 1996), and genetic variation acting through an organism's developmental framework can generate “structured” or “constrained” pleiotropy (de Jong, 1990 and Wagner, 1989). At the same time, genes with different combinations of pleiotropic effects offer opportunities for genetic correlations, and thus the trajectory of adaptive evolution, to change over time (Lande, 1980 and Wagner, 1989). A

causal trait network provides a mechanistic set of constraints on pleiotropic effects but, as our simulations show, the resulting genetic correlation patterns can be strongly influenced by the particular network nodes that are the direct targets of large-effect QTLs. Trait network simulations in which genetic variation directly affecting individual traits is modeled as random effects, rather than fixed effects as we have done, may be useful for testing network effects on **G**-matrix stability in a population context.

4.2. Utility of life-history trait networks

The availability of analytical tools to test trait network models that include QTLs provides opportunities both to test the validity of such models as explanations for life-history trait correlations and to predict which traits are the direct targets of QTL effects. Identifying where and when effects of genetic variation occur in development will be a critical step in developing a unified understanding of the evolution of form and life histories (Pigliucci, 2007 and Schlichting and Pigliucci, 1998). SEM analysis results provided highly specific support for the correct model, and the best-fitting model presented a reasonable approximation of the correct causal relationships between QTL and traits even when only four of the simulated traits were included as measured variables. The abbreviated model, however, was incorrect in some details, due both to the incomplete measurement data and degrees-of-freedom limitations. Correctly distinguishing direct vs. indirect QTL effects on traits, and thus obtaining useful insights on the functional basis for developmental variation, is likely to depend on relatively detailed data on traits representing nodes in the causal structure.

Realistically, most empirical studies will not measure all traits in a hypothesized developmental network. Moreover, some measured traits are likely to be only indirect measures of the “true” nodes in a causal QTL-trait network. For these reasons, our abbreviated SEM structure is probably a more realistic example of both the capabilities and limitations of SEM or other empirical approaches to trait network analysis.

Exploratory algorithms that made no *a priori* assumptions about the network structure (other than constraining QTLs to be strictly causal) identified several networks with strong statistical support, with varying degrees of similarity to the actual network. Exploratory network algorithms that incorporate QTLs have been proposed as tools for inferring causal trait networks (e.g. Chaibub Neto et al., 2008 and Liu et al., 2008). Our results suggest that exploratory methods may provide evidence for the overall structure of the true QTL-trait network but are likely to be incorrect in many details. Factors such as heterogeneous measurement errors, environmental or developmental heterogeneity in sample populations, and some patterns of pleiotropy in QTL effects may also favor models that are incorrect and even ones that are clearly implausible from a biological standpoint (Remington, 2009 and Rockman, 2008). Exploratory path analysis approaches may be highly useful when there is uncertainty over causal structures, but some attempt at *a priori* identification of biologically reasonable paths is warranted when

such methods are used (Shipley, 1997). Further experimental verification of model predictions from empirical studies is also clearly warranted.

A number of recent studies have used quantitative approaches to investigate the mechanistic basis for developmental variation (Jamniczky and Hallgrímsson, 2009, Márquez, 2008, Salazar-Ciudad and Jernvall, 2002, Tonsor and Scheiner, 2007 and Willmore et al., 2007). From a quantitative genetics perspective, several proposed models to explain correlated traits and resource allocation trade-offs have used bifurcating networks to represent developmental hierarchies (Björklund, 2004, de Jong, 1993, Slatkin, 1987 and Worley et al., 2003). The use of path models instead of simple bifurcating models offers the additional flexibility of accommodating more complex reticulating relationships between traits, which is often predicted in theoretical models of life-history evolution (Byers, 2005, Johnson et al., 2008, Kingsolver and Schemske, 1991, Mitchell-Olds and Bergelson, 1990, Scheiner et al., 2000, Shipley, 1997, Tonsor and Scheiner, 2007 and Weis and Kapelinski, 1994). In adding QTL effects to a path model framework, the modeling approach we have used is similar to those being used in "systems genetics" studies to model the integration of QTL effects with gene regulatory networks (Liu et al., 2008, Mackay et al., 2009, Rockman, 2008, Schadt et al., 2005 and Zhu et al., 2004), which can be extended to other traits that form interacting networks (Chaibub Neto et al., 2008, Li et al., 2006 and Remington, 2009).

The utility of trait networks also depends on the degree to which the hypothesized networks actually shape patterns of multiple-trait variation. Trait correlations in data simulated under the trait network models showed a significant degree of similarity with those from field data despite the fact that the simulated path coefficients were arbitrary except for their sign. This indicates that a causal network with the overall structure used for our simulations is a plausible explanation for observed trait variation patterns in *A. lyrata*. Furthermore, models that incorporated QTL effects on traits known to differ between the two parental populations of the F_2 family (*VS* and *VS+SilS* models) generated the strongest correlations with data from both the Greensboro and Norway field sites. The Greensboro data by themselves do not provide a rigorous test of the trait network, as some aspects of the model were based in part on observations from the Greensboro study site, and the model scenarios were developed with prior knowledge of the Greensboro correlation structure. Data from the Norway site, however, provide stronger support for the model because data from the Norway study site were not available to us when the model scenarios were developed. In addition, the consistency between the Norway and Greensboro phenotypic correlations in these widely different environments suggests that the correlation patterns have a common developmental basis. This supports the hypothesis that these patterns are indeed shaped by cause-effect relationships between developmental traits. Nevertheless, it must be borne in mind that many different causal mechanisms could possibly result in very similar patterns of genetic and phenotypic trait correlations, but with distinctly different implications in terms of selective response (Gromko, 1995 and Houle, 1991). This may be of special concern when the set of measured traits is incomplete, as in our case.

Genetic marker data have been assayed for the F_2 populations from the Norway and Greensboro study sites in our example, so QTL analyses can be used for further tests of model predictions. In particular, the close fit of models with QTL effects on vegetative meristem allocation, including pleiotropic effects on siliques per shoot in the Greensboro environment, provides hypotheses that can be tested in QTL analyses. Further studies in which data from segregating crosses are collected on all traits used in the model would provide more definitive tests. Finally, the model could be extended to predict effects of resource allocation traits and the underlying QTLs on survival over multiple years in different environments, and tested in multiple environments to evaluate how variation in life history traits contributes to local adaptation.

In summary, trait network models such as the one we have developed show promise for integrating theoretical aspects of life history variation and evolution with empirical data. They provide a causal framework for understanding the functional basis of phenotypic and genetic trait correlations and their consequent effects on evolutionary trajectories, and can be tested using QTL studies. This modeling approach is not limited to any particular organism, but can be flexibly adapted to a variety of plant and animal developmental processes and life histories.

Acknowledgments

The authors thank Outi Savolainen and Päivi Leinonen for providing the data from the Norway field study site and for constructive suggestions on the manuscript, and four anonymous reviewers whose suggestions have greatly improved the manuscript. Support for undergraduate research on this project was funded by National Science Foundation Grants 0634182 (R.G., R.E., J.R. and D.L.R), 0850465 (W.C., N.Z., J.R. and D.L.R), and 0926288 (J.R. and D.L.R.).

Appendix A. Genetic and environmental correlations under a two-trait developmental hierarchy

As described in the text of the paper, developmental hierarchies or networks introduce trait correlations that are not readily explained by the multivariate partitioning between genetic and non-genetic (or environmental) sources of variance (Atchley and Hall, 1991). Developmental networks will lead to both genetic and environmental correlations even when both direct pleiotropy (as defined in the text) and direct common-environment effects are absent. Moreover, the trait network will induce correlations between genetic and environmental correlation (or covariance) matrices themselves because the two matrices are influenced by the same causal factors.

As a simple example, consider a situation in which variation in a trait (T_1) expressed early in development affects the value of a second trait (T_2) expressed later in development, with means μ_1 and μ_2. Assume that variation in each trait is directly affected by independent sets of genes, with effects g_1 and g_2, and independent environmental effects e_1 and e_2; i.e. functional pleiotropy and correlation of the environmental effects are both absent. Let b_{12} be the partial regression coefficient of the effect of T_1 on T_2. Thus, linear models for T_1 and T_2 in individual i can be expressed as follows:

equation(A1a)

$T_{1i}=\mu_1+g_{1i}+e_{1i}$

and

equation(A1b)

$T_{2i}=\mu_2+g_{2i}+b_{12}(T_{1i}-\mu_1)+e_{2i}$

with variances:

equation(A2a)

$$\sigma^2_{1P}=\sigma^2_{1G}+\sigma^2_{1E}$$

and

equation(A2b)

$$\sigma^2_{2P}=\sigma^2_{2G}+b^2_{12}(\sigma^2_{1G}+\sigma^2_{1E})+\sigma^2_{2E}$$

and the covariance between T_1 and T_2 is

equation(A2c)

$$\sigma_{12P}=b_{12}(\sigma^2_{1G}+\sigma^2_{1E})$$

where σ^2_G and σ^2_E are the "direct" genetic and environmental variances associated with *gi* and *ei*, respectively.

The total genetic variance for T_2 (which we designate σ^{2*}_{2G}) includes not only the direct genetic variance σ^2_{2G} but also the indirect effect of the genetic variance in T_1 on T_2. Thus

equation(A3a)

$$\sigma^{2*}_{2G}=\sigma^2_{2G}+b^2_{12}\sigma^2_{1G}$$

and similarly

equation(A3b)

$$\sigma^{2*}_{2E}=\sigma^2_{2E}+b^2_{12}\sigma^2_{1E}$$

The effects of T_1 on T_2 result in a phenotypic correlation between the two traits, in spite of the independence of both the direct genetic and environmental effects on the traits, as follows:

equation(A4)

$$r_{12P} = b_{12}\frac{\sigma_{1P}}{\sqrt{b_{12}^2\sigma_{1P}^2+\sigma_{2P}^2}} = b_{12}\frac{\sqrt{\sigma_{1G}^2+\sigma_{1E}^2}}{\sqrt{b_{12}^2(\sigma_{1G}^2+\sigma_{1E}^2)+\sigma_{2G}^2+\sigma_{2E}^2}}$$

The genetic and environmental correlations ($r_{12}G$ and $r_{12}E$, respectively) are obtained by including only the variances associated with the direct genetic and environmental components of the respective traits from Eq.(A4). Specifically:

equation(A5a)

$$r_{12G} = b_{12}\frac{\sqrt{\sigma_{1G}^2}}{\sqrt{b_{12}^2\sigma_{1G}^2+\sigma_{2G}^2}}$$

and

equation(A5b)

$$r_{12E} = b_{12}\frac{\sqrt{\sigma_{1E}^2}}{\sqrt{b_{12}^2\sigma_{1E}^2+\sigma_{2E}^2}}$$

Note that the signs of $r_{12}P$, $r_{12}G$, and $r_{12}E$ are all the same as that of b_{12}, which will result in a degree of concordance between the genetic and environmental correlations. The strength of this relationship will depend on the magnitude of the path coefficient and the ratios of σ_G^2 to σ_E^2 for the two traits. In the extreme case where the ratios of σ_G^2 to σ_E^2 are the same for both traits, the phenotypic, genetic, and environmental correlations will all be identical.

None of the above should be taken to suggest that genetic and environmental variances and covariances cannot be partitioned under a causal network model. Genetic and environmental components remain separable based on the origin of the variation, whether in upstream or downstream traits, as the above equations make clear. However, the genetic and environmental covariances (or covariance matrices in the extension to more than two traits) will be correlated because they share b_{12} terms in the equations above. If the direct environmental effects on the two traits (e_1 and e_2) were correlated (i.e. common environmental effects in the usual sense), or if the direct genetic effects were correlated (i.e. “direct” pleiotropy), the path-induced correlations could be reinforced, weakened, or counteracted depending on the signs and the magnitudes of the direct-effects' correlations. Furthermore, in more complex models including more traits, covariances between traits could be either reinforced or weakened by the coefficients of multiple paths connecting pairs of traits, as discussed elsewhere in the paper.

Appendix B. Reasoning for Trait Network Paths

Here we describe in detail the rationale for each predicted causal relationship among the developmental and life history traits in *A. lyrata* that are depicted in the trait network model.

Allocation of meristems, which was simulated using Eqs. (2a), (2b) and (2c), is described first, followed by the remaining allocation pathways depicted by linear equations (Eq. (1)).

B.1. Meristem allocation paths

Axillary meristems develop on the upper side of each node where the base of a leaf intersects with the vegetative shoot (i.e. the leaf axil). We are here concerned specifically with the number and alternate fates of axillary meristems in the unelongated vegetative (pre-flowering) portion of the primary shoot. It is assumed that lateral vegetative shoots do not generally switch to become reproductive during the same growing season, but it seems likely that this would occasionally happen in reality. Thus, a Poisson rather than binomial model was used to simulate numbers of vegetative and reproductive shoots, which allows for a non-zero probability that the number of lateral vegetative plus reproductive shoots could exceed the total number of axillary meristems.

$M \rightarrow V_S$

Increasing the total number of axillary meristems proportionately increases the number of meristems available to become lateral vegetative shoots.

$M \rightarrow R_S$

Increasing the total number of axillary meristems proportionately increases the number of meristems available to become reproductive shoots.

$V_S \rightarrow R_S$

An increase in the proportion of axillary meristems that develop as lateral vegetative shoots results in a proportionate reduction in the number of remaining axillary meristems potentially available to develop as reproductive shoots.

B.2. Paths in linear equations

$V_S \rightarrow D1$

The plant has a limited amount of resources for lateral vegetative development. There is a tradeoff between number of lateral vegetative shoots and the diameter of leaves growing from vegetative shoots, thus leading to reduced rosette diameter on plants with more lateral vegetative shoots.

$V_S \rightarrow dD$

Loss of rosette diameter from the death of older leaves is counteracted by the growth of new leaves from vegetative shoots. Moreover, vegetative shoots increase the rate of resource acquisition during the reproductive period through photosynthesis. The resources gained from photosynthesis can be used to increase the plant's rosette diameter.

M→TD*1*

Total number of meristems is a component of the plant's pre-reproductive resource acquisition, and allows for an increased amount of resources produced through photosynthesis. This increases the amount of photosynthate stored in roots, resulting in a larger taproot.

V_S→Sen

More vegetative shoots increase the amount of resource acquisition through photosynthesis. This lessens the need to recycle photosynthate in leaves through senescence as an alternate source of resources to produce other tissues.

V_S→SilS

More vegetative shoots increase the net amount of available resources through photosynthesis. These resources can be used to increase the number of siliques per reproductive shoot.

R_S→dD

The more resources allocated to making reproductive shoots, the fewer resources there are for increasing rosette diameter. Thus, increasing the number of reproductive shoots leads to a greater decrease or a lesser increase in rosette diameter during the reproductive season.

R_S→SilS

The more resources allocated to making reproductive shoots, the fewer resources there are for producing flowers and ripening siliques on these shoots, thus reducing the number of siliques per shoot.

R_S→Sen

Allocating more resources to producing reproductive shoots leads to a decrease in resources available for producing other tissues. To replace these used resources, increased senescence of leaves will occur in order to recycle the photosynthate they contain for other uses. Thus, an increase in reproductive shoots leads to an increased rate of senescence.

Sen→SilS

Senescence of leaves recycles resources that can be used for producing other tissues. These resources can be used to develop more siliques per shoot.

Sen→dD

Senescence results in loss of leaves from the plant's rosette. This leads to a net decrease in rosette growth during the reproductive season.

SilS→Sen

Allocating more resources to flowering and silique ripening leads to a decrease in resources available for producing other tissues. To replace these used resources, increased senescence of leaves will occur in order to recycle the photosynthate they contain for other uses. Thus, an increase in the number of siliques per shoot leads to an increased rate of senescence.

D*1*→SilS

A larger pre-flowering rosette diameter is one component of pre-reproductive resource acquisition, and allows for an increased amount of resources produced through photosynthesis. The increase in resources from photosynthesis can in turn be used to increase the number of siliques per shoot.

D*1*→TD*1*

A larger pre-flowering rosette diameter is one component of pre-reproductive resource acquisition, and allows for an increased amount of resources produced through photosynthesis. This increases the amount of photosynthate stored in roots, resulting in a larger pre-reproductive taproot.

dD→TD*2*

A greater net increase or reduced net decrease in rosette diameter results in a larger post-reproductive rosette diameter and allows for an increased amount of resources produced through photosynthesis. This increases the amount of photosynthate stored in roots, resulting in a larger taproot at the end of the reproductive season.

TD*1*→SilS

The taproot is used for storing photosynthate. An increased pre-reproductive taproot diameter thus represents increased resource storage. These resources can be used to produce more siliques per shoot.

TD*1*→Sen

An increased pre-reproductive taproot diameter represents increased resource storage. Senescence of leaves is also used to recycle resources for other uses, so a larger taproot lessens the need for senescence.

TD*1*→TD*2*

A larger initial taproot leads to a larger final taproot.

B.3. Paths affecting fitness traits (not explicitly modeled in this study)

V_S→Survival

More vegetative shoots increase the amount of resource acquisition through photosynthesis. This leads to more resource allocation to plant maintenance, resulting in a higher survival rate.

Sen→Survival

Senescence of leaves leads to a decrease in the number of leaves available for photosynthesis. A lower photosynthesis rate leads to a lower resource acquisition rate, which results in a lower survival rate. Therefore, a higher senescence rate causes a lower survival rate.

TD*1*→Survival

An increased pre-reproductive taproot diameter represents increased resource storage, which results in an increased amount of available resources for plant maintenance. This leads to a higher survival rate.

dD→Survival

A greater net increase or reduced net decrease in rosette diameter results in a larger post-reproductive rosette diameter and allows for an increased amount of resources produced through photosynthesis. This results in more available photosynthetic resources for plant maintenance, and leads to a higher survival rate.

R_S→Reproduction

An increased number of reproductive shoots leads to an increase total silique and seed production, and thus greater reproductive output.

SilS→*Re*production

An increased number of siliques per shoot leads to greater seed production, and thus a greater reproductive output.

References

Akaike, H., 1974. A new look at the statistical identification model. IEEE Trans.

Autom. Control 19, 716–723.

Akaike, H., 1987. Factor analysis and AIC. Psychometrika 52, 317–332.

Arnold, S.J.,B¨ urger, R.,Hohenlohe,P.A.,Ajie,B.C.,Jones,A.G.,2008.Understanding the evolutionandstabilityoftheG-matrix.Evolution62,2451–2461.

Atchley, W.R.,Hall,B.K.,1991.A model for development and evolution of complex morphological structures.Biol.Rev.66,101–157.

Björklund, M.,2004.Constancyofthe G matrix inecologicaltime.Evolution58, 1157–1164.

Byers, D.L.,2005.Evolution in heterogeneous environments and the potential of maintenance of genetic variationin traits of adaptive significance. Genetica 123, 107–124.

Chaibub Neto,E.,Ferrara,C.T.,Attie,A.D.,Yandell,B.S.,2008.Inferringcausal phenotype networksfromsegregatingpopulations.Genetics179,1089–1100.

Cheverud, J.M.,1996.Quantitativegeneticanalysisofcranialmorphologyinthe cotton-top (Sanguinus oedipus) andsaddleback(S. fuscicollis) tamarins.J.Evol. Biol. 9,5–42.

Cheverud, J.M.,Marroig,G.,2007.Comparingcovariancematrices:random skewers method compared to the common principal components model. Genet. Mol.Biol.30,461–469.

Cheverud, J.M.,Rutledge,J.J.,Atchley,W.R.,1983.Quantitativegeneticsofdevel- opment: genetic correlations among age-specific trait values and the evolution of ontogeny.Evolution37,895–905.

Clauss, M.J.,Koch,M.A.,2006.Poorlyknownrelativesof Arabidopsis thaliana. Trends PlantSci.11,449–459.

Crespi, B.J.,Bookstein,F.,1989.Apath-analyticmodelforthemeasurementof selection onmorphology.Evolution43,18–28.

de Jong,G.,1990.Quantitativegeneticsofreactionnorms.J.Evol.Biol.3,447–468.

de Jong,G.,1993.Covariancesbetweentraitsderivingfromsuccessiveallocations of aresource.Funct.Ecol.7,75–83.

de Jong,G.,vanNoordwijk,A.J.,1992.Acquisitionandallocationofresources: genetic (co)variances,selection,andlifehistories.Am.Nat.139,749–770.

Fox, J.,2006. Structural equation modeling with the sem package in R.Struct. Equation Modeling13,465–486.

Gromko, M.H.,1995. Unpredictability of correlated response to selection :pleio- tropy andsamplinginteract.Evolution49,685–693.

Hegmann, J.P.,DeFries,J.C.,1970.Are genetic correlations and environmental correlations correlated?Nature226,284–286.

Houle, D.,1991. Genetic covariance of fitness correlates: what genetic correlations are madeofandwhyitmatters.Evolution45,630–648.

Jamniczky, H.A.,Hallgrímsson, B.,2009.Acomparisonofcovariancestructurein wild andlaboratorymuroidcrania.Evolution63,1540–1556.

Johnson, J.B.,Burt,D.B.,DeWitt,T.J.,2008.Form,function,andfitness:pathwaysto survival. Evolution62,1243–1251.

Kelly, J.K.,2009. Connecting QTLstotheG-matrixofevolutionaryquantitative genetics. Evolution43,813–825.

Kingsolver, J.G.,Schemske,D.W.,1991.Pathanalysesofselection.TrendsEcol. Evol. 6,276–280.

Koelewijn, H.P.,2004.Rapid change in relative growth rate between the vegetative and reproductive stage of the life cycle in Plantago coronopus. NewPhytol.163, 67–76.

Lacey, E.P.,Herr,D.,2005.Phenotypicplasticity,parentaleffects,andparental care inplants? I.An examination of spike reflectance in Plantago lanceolata. Am. J.Bot.92,920–930.

Lande, R.,1979.Quantitativegeneticanalysisofmultivariateevolution,appliedto brain:body sizeallometry.Evolution33,402–416.

Lande, R.,1980.Thegeneticcovariancebetweencharactersmaintainedby pleiotropic mutations.Genetics94,203–215.

Lande, R.,Arnold,S.J.,1983.Themeasurementofselectiononcorrelatedchar- acters. Evolution37,1210–1226.

Leinonen, P.H.,Remington,D.L.,Savolainen,O.,2011.Localadaptation,phenotypic differentiation and hybrid fitness in diverged natural populations of Arabi-dopsis lyrata. Evolution65,90–107.

Leinonen, P.H., Sandring, S., Quilot, B., Clauss, M.J., Mitchell-Olds, T., ˚ Agren, J.,2009. Local adaptation in European populations of Arabidopsis lyrata (Brassicaceae). Am. J.Bot.96,1129–1137.

Li, R.,Tsaih,S.-W.,Shockley,K.,Stylianou,I.M.,Wergedal,J.,Paigen,B.,Churchill, G.A., 2006.Structuralmodelanalysisofmultiplequantitativetraits.PLoS Genet. 2,e114.

Liu, B.,delaFuente,A.,Hoeschele,I.,2008.Genenetworkinferenceviastructural equation modelingingeneticalgenomicsexperiments.Genetics178, 1763–1776.

Lynch, M.,Walsh,B.,1998.GeneticsandAnalysisofQuantitativeTraits.Sinauer, Sunderland, MA. Mackay, T.F.C.,Stone,E.A.,Ayroles,J.F.,2009.Thegeneticsofquantitativetraits: challenges andprospects.Nat.Rev.Genet.10,565–577.

Márquez, E.J.,2008.Astatisticalframeworkfortestingmodularityinmulti- dimensional data.Evolution62,2688–2708. MathWorks Inc.,2007.MatLab,version7.4.

Mitchell-Olds, T.,Bergelson,J.,1990.Statisticalgeneticsofanannualplant, Impatiens capensis. II. Naturalselection.Genetics124,417–421.

Mitteroecker, P.,Bookstein,F.,2007.Theconceptualandstatisticalrelationship between modularityandmorphologicalintegration.Syst.Biol.56,818–836.

Phillips, P.C.,1997.CPC—Common Principal Component Analysis Program. Pigliucci, M.,2005.Evolutionofphenotypicplasticity:wherearewegoingnow? Trends Ecol.Evol.20,481–486.

Pigliucci, M.,2007.Doweneedanextendedevolutionarysynthesis?Evolution61, 2743–2749.

R DevelopmentCoreTeam,2008.R:A language and Environment for Statistical Computing. R Foundation for Statistical Computing, Vienna, Austria.

Remington, D.L.,2009.Effectsofgeneticandenvironmentalfactorsontrait network predictionsfromquantitativetraitlocusdata.Genetics181, 1087–1099.

Riihimäki, M.,Podolsky,R.,Kuittinen,H.,Koelewijn,H.,Savolainen,O.,2005. Studying genetics of adaptive variation in model organisms: flowering time variation in Arabidopsis lyrata. Genetica123,63–74.

Rockman, M.V.,2008.Reverse engineering the genotype–phenotype map with natural geneticvariation.Nature456,738–744.

Roff, D.A.,1997.Evolutionary Quantitative Genetics. Chapman and Hall, New York. Salazar-Ciudad, I.,Jernvall,J.,2002.Agenenetworkmodelaccountingfor development and evolution of mammalian teeth. Proc.Natl.Acad.Sci.USA 99, 8116–8120.

Schadt, E.E.,Lamb,J.,Yang,X.,Zhu,J.,Edwards,S.,GuhaThaktura,D.,Sieberts,S.K., Monks, S.,Reitman,M.,Zhang,C.,Lum,P.Y.,Leonardson,A.,Thieringer,R., Metzger, J.M.,Yang,L.,Castle,J.,Zhu,H.,Kash,S.F.,Drake,T.A.,Sachs,A., Lusis, A.J.,2005.Anintegrativegenomicsapproachtoinfercausalassociations between geneexpressionanddisease.Nat.Genet.37,710–717.

Scheiner, S.M.,Mitchell,R.J.,Callahan,H.S.,2000.Usingpathanalysistomeasure natural selection.J.Evol.Biol.13,423–433.

Schlichting, C.D.,Pigliucci,M.,1998.PhenotypicEvolution:AReactionNorm Perspective. Sinauer, Sunderland,MA. Shipley, B.,1997.Exploratory pathanalysis with applications in ecologyand evolution. Am.Nat.149,1113–1138.

Slatkin, M.,1987.Quantitative genetics of heterochrony.Evolution41,799–811.

Spirtes, P.,Glymour,C.,Scheines,R.,2000.Causation,Prediction,andSearch,2nd ed. MITPress,Cambridge,MA.

Stearns, S.,deJong,G.,Newman,B.,1991.Theeffectsofphenotypicplasticityon genetic correlations.TrendsEcol.Evol.6,122–126.

Stearns, S.C.,1992.The Evolution of Life Histories. Oxford University Press, Oxford.

Steppan, S.J.,Phillips,P.C.,Houle,D.,2002.Comparativequantitativegenetics: evolution of the G matrix. TrendsEcol.Evol.17,320–327.

Tonsor, S.J.,Scheiner,S.M.,2007.PlastictraitintegrationacrossaCO2 gradient in Arabidopsis thaliana. Am.Nat.169,E119–E140.

van Noordwijk,A.J.,deJong,G.,1986.Acquisitionandallocationofresources:their influence onvariationinlifehistorytactics.Am.Nat.128,137–142.

Wagner, G.P.,1989.Multivariatemutation–selection balance with constrained pleiotropic effects.Genetics122,223–234.

Wang, R.,Farrona,S.,Vincent,C.,Joecker,A.,Schoof,H.,Turck,F.,Alonso-Blanco,C., Coupland, G.,Albani,M.C.,2009. PEP1 regulates perennial flowering in Arabis alpina. Nature459,423–428.

Weis, A.E.,Kapelinski,A.,1994.Variableselectionon Eurosta's gallsize.II.Apath analysis oftheecologicalfactorsbehindselection.Evolution48,734–745.

Willmore, K.E.,Young,N.M.,Richtsmeier,J.T.,2007.Phenotypicvariability:its components, measurement and underlying developmental processes. Evol. Biol. 34,99–120.

Worley, A.C.,Houle,D.,Barrett,S.C.H.,2003.Consequencesofhierarchicalalloca- tion fortheevolutionoflife-historytraits.Am.Nat.161,153–167.

Wright, S.,1918.Onthenatureofsizefactors.Genetics3,367–374. Wright, S.,1921.Correlationandcausation.J.Agric.Res.20,557–585.

Zhu, J.,Lum,P.Y.,Lamb,J.,GuhaThaktura,D.,Edwards,S.W.,Thieringer,R., Berger, J.P.,Wu,M.S.,Thompson,J.,Sachs,A.B.,Schadt,E.E.,2004.An integrative genomics approach to there construction of gene networks in segregating populations.Cytogenet.GenomeRes.105,363–374.